Electric Birefringence Measurements Of Native, Denatured, and Renatured Xanthan

GREGORY J. BESIO, IAN M. LEAVESLEY, and ROBERT K. PRUD'HOMME, *Department of Chemical Engineering, Princeton University, Princeton, New Jersey 08544,* and RAYMOND FARINATO, *American Cyanamid, Central Research Laboratories, Stamford, Connecticut*

Synopsis

Electric birefringence measurements were performed on three xanthan solutions to determine conformational differences between native xanthan, denatured xanthan (heated in 4*M* urea to 90°C and cooled), and renatured xanthan (heated and cooled). The birefringence of samples exposed to pulses of 1000 V for 1 ms were analyzed to determine longest relaxation times and steady-state birefringence. The results showed the following order for steady state birefringence, native > renatured > denatured, and longest relaxation time, renatured > native > denatured. The results are interpreted in terms of helix reformation and aggregation upon renaturing.

INTRODUCTION

Xanthan polysaccharide solutions have unique rheological properties that include insensitivity to solution ionic strength, resistance to shear degradation, and stability at elevated temperatures in brine.[1-10] These properties result from the molecular configuration of the xanthan molecule. While it is agreed that the xanthan backbone is a helix, which makes xanthan a semi-rigid, rodlike molecule, there is considerable debate as to exact structure of the helix. Several researchers have proposed that xanthan exists as a fivefold single-stranded helix, and support this contention with evidence obtained from X-ray diffraction,[11] by matching molecular models to the results of intrinsic viscosity and light scattering experiments,[12] or by considering the concentration dependence of the order/disorder transition.[2] However, several researchers contend that xanthan exists as a double stranded helix. Evidence for this view comes from electron microscopy,[13] light scattering,[14] and light scattering in two different solvents.[15,16] The arguments for the single and double stranded helix conformation are well presented in the recent articles by Sato et al.[15,16]

The evidence that xanthan exists as a helix comes from X-ray diffraction measurements on solid samples[11] and from measurements of optical rotary dispersion (ORD) and circular dichroism (CD).[2,8,9,14,17] These studies show that xanthan undergoes a transition from an ordered helical conformation (native xanthan) to a disordered conformation (denatured xanthan) as temperature is raised, and that the temperature of this transition increases with increasing solution ionic strength. Figure 1, from Milas and Rinaudo,[2] shows

Journal of Applied Polymer Science, Vol. 33, 825–834 (1987)
 CCC 0021-8995/87/030825-10$04.00

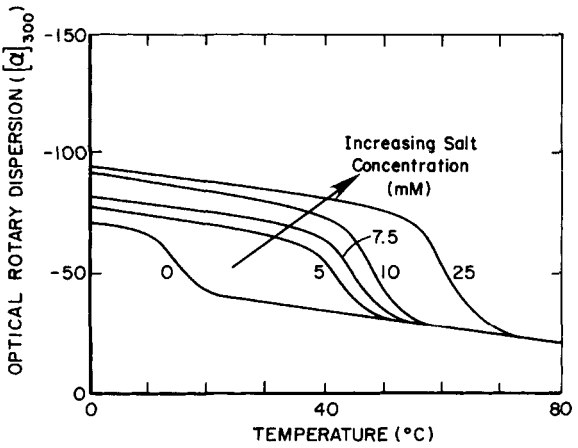

Fig. 1. Specific rotation, $[\alpha]_{300}$, as a function of temperature for different salt (NaCl) concentrations (reproduced from Ref. 2 with permission).

ORD results for xanthan as a function of temperature and ionic strength. It is reported that the transition is completely reversible (renatured xanthan) and shows no hysteresis,[2] in the ORD response.

In this paper we present results from electric birefringence measurements on native, denatured, and renatured xanthan solutions. Both the steady state birefringence and the field-free relaxation times support the contention that native xanthan has a double-helix or rigid dimer structure.

EXPERIMENTAL

Apparatus

The electric birefringence apparatus is based on a design suggested by O'Konski,[24] and is illustrated schematically in Figure 2. The light source is a Melles Griot Model LHP 111 HeNe laser (Melles Griot, San Marcos, CA) of wavelength 632.8 nm. The detection electronics are based on a simple photodiode (UV-100B, EG & G Electro-Optics, Salem, MA) and operational amplifier circuit. The output from the detector circuit was recorded on a 2MHz Nicolet

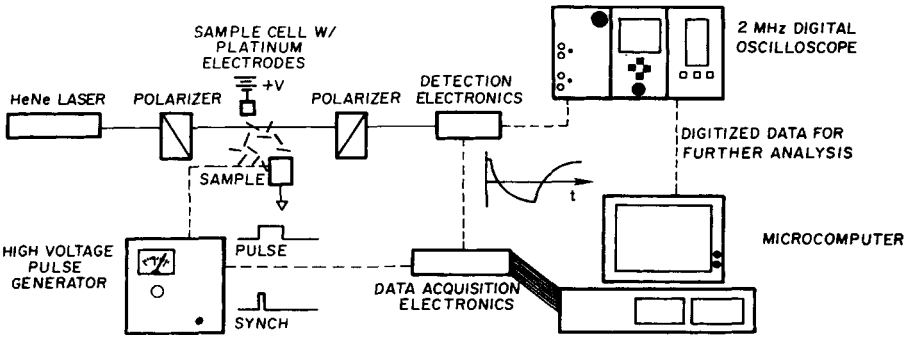

Fig. 2. Electric birefringence apparatus.

4094 Digital Oscilloscope (Nicolet Instrument, Co., Madison, WI). Data recorded on the scope could be plotted directly on an HP 7470 $x-y$ plotter (Hewlett Packard, Palo Alto, Ca) or transferred to an IBM PC personal computer (IBM Corp., Boca Raton, FL) for analysis. The electrodes were platinum, and were separated by a gap of 3 mm in a cell with a path length of 10 mm. Electric fields were generated using a Cober 605P (Cober Electronics, Stamford, CT) high voltage pulse generator. Pulses of 0-2 kV could be generated with durations varying from 0 to 5 ms.

MATERIALS

A concentrated xanthan solution was obtained from Pfizer Inc. (Flocon 4800 C, Pfizer Inc., Groton, CT) which contained 13.8 wt % xanthan. The solution was obtained directly from the fermentation broth and was relatively free of residual cellular debris.[5,18,19] The xanthan sample, never having been dried, was reported to have no "micro gel" aggregates.[5,18,19] A xanthan that had been dried using heat would undergo denaturation as reported by Holzwarth and Prestridge[13] and might have a different backbone configuration upon dissolution than a sample that had never been dried. The change in backbone configuration suggested by Holzwarth would be the introduction of defects in the double-helix backbone, leading to a more flexible molecule.

The concentrated xanthan solution was diluted with deionized water to 100 ppm to produce a dilute solution. Sodium azide was added as a bacteriocide to all solutions (3 mM). Three samples denoted "native xanthan," "denatured xanthan," and "renatured xanthan" were prepared as described below. The "native xanthan" was the diluted solution described above. The "renatured" sample was obtained by heating the diluted xanthan to 90°C and then allowing it to cool to room temperature. Measurements of ORD by Rinaudo and Milas[2,3] or Holzwarth[17] show that heating a xanthan solution in 3 mM salt to 90°C induces an order/disorder transition in the polymer chain; it denatures. Upon cooling the ORD signal returns to its original value, indicating that the material has renatured. The "denatured xanthan" sample was obtained by adding $4M$ urea to the native xanthan and heating the sample to 90°C. Jamieson et al.[20] have shown that $4M$ urea prevents the renaturing of xanthan and keeps it in the disordered (denatured) state.

DATA ANALYSIS

The steady state birefringence Δn_{ss} was determined from the maximum value of the detector response as shown in Figure 3. The longest relaxation time τ_1 was obtained from an analysis of the field-free decay of the orientation after the end of the voltage pulse. The relaxation was assumed to follow a sum of exponentials:[21]

$$\Delta n(t) = A_1 e^{-t/\tau_1} + A_2 e^{-t/\tau_2} + \cdots \tag{1}$$

with τ_1 being the longest relaxation time. For flexible and semiflexible molecules this normal-mode analysis gives information about the overall size and stiffness of the polymer chain.[21] The field-free relaxation portion of the curves were plotted as the logarithm of the detector response vs. time, as shown in

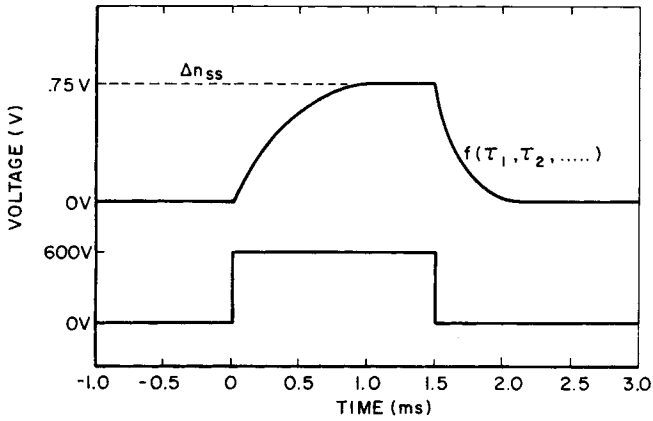

Fig. 3. Schematic representation of electric birefringence response (upper curve) showing orientation, steady state birefringence (Δn_{ss}), and relaxation; lower curve shows imposed voltage.

Figure 4 for some representative data. The long-time portion of the curve was fitted with a straight line as shown in Figure 4 to obtain the longest relaxation time (see Appendix A for data reduction analysis). The slope of the line is $-(2/\tau_1)$.

Other authors[22,23] have analyzed birefringence data by looking at the initial slope of the relaxation curves (i.e., at $t = 0$) rather than the long-time behavior. For rigid rods or stiff molecules with persistence lengths nearly equal to the contour length analyzing the short-time relaxation is appropriate. Analyses show that the initial slope provides average length information for rods and local stiffness information for very stiff molecules.[24] However, for

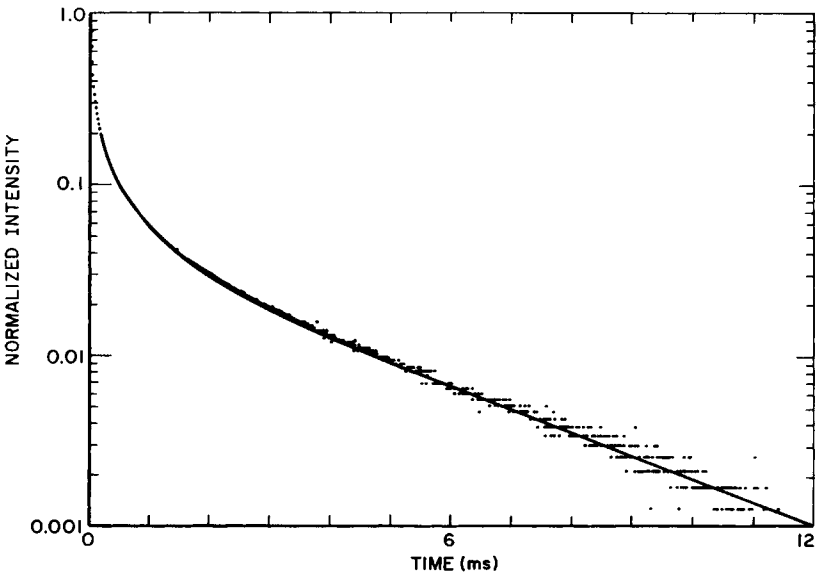

Fig. 4. Detector intensity versus time for a xanthan solution in deionized water at 25°C. The longest relaxation time is obtained from the slope of the curve at long times. The solid line is a sum-of-exponentials fit to the data.

TABLE I
Relaxation Times for Xanthan

	τ_1(ms)	Δn_{ss} (rad $\times 10^9$)
Native	1.70	7.62
Denatured	1.20	3.12
Renatured	2.02	5.67

molecules with contour lengths greater than several persistence lengths, normal mode analysis[21] shows that the relaxation of the molecule is given by a series of exponentials [eq. (1)] with the number of terms in the series equal to twice the contour length L divided by the persistence length, l_p. Sato's data show that $L/l_p \sim 10$ for xanthan; consequently, 20 exponentials would be required. The shorter relaxation times become closely spaced, and therefore, at $t = 0$ most of the modes contribute to the observed relaxation. It is not possible to decompose the initial relaxation behavior and obtain fundamental molecular parameters for flexible and semiflexible molecules.

RESULTS

Pulses of 1000 V (330 kV/m) for 1 ms were used to achieve steady-state birefringence in all samples. This value of applied field gave strong birefringence so that signal/noise ratios were high enough to give resolution of the entire decay curve. The analysis of the relaxation curves are presented in Table I. The longest relaxation time for the denatured xanthan, $\tau_1 = 1.20$ ms, is shorter than the relaxation time for the native xanthan, $\tau_1 = 1.70$ ms. This is consistent with the denatured material being collapsed into a more compact configuration. Surprisingly the longest relaxation time of the renatured sample, $\tau = 2.02$ ms, is longer than the relaxation time for the native xanthan. This suggests a larger aggregate has been formed by the incorporation of multiple xanthan strands during renaturing or renaturing out of register to create a longer species. This phenomena has recently been corroborated by Sato et al.[16] Their Figure 5 shows that xanthan renatured in semidilute solution had a higher intrinsic viscosity than that of the native xanthan—the xanthan reforms into large aggregates. Our solutions have been renatured at 100 ppm—above the critical overlap concentration defining the boundary of the simidilute region. For this xanthan the critical overlap concentration was $C^* = 40$ ppm ($\equiv 0.7/[\eta]$), where $[\eta]$ was measured with a Contraves Low Shear Viscometer at shear rates below 1 s^{-1}.[25] However, as Sato's data shows, xanthan renatured in *very* dilute solutions (i.e., below C^*) had a lower intrinsic viscosity than the native xanthan. A xanthan strand reforming a dimer structure with no other neighbors to interact with will coil back upon itself to form a more compact molecule. These transformations are shown schematically in Figure 5. This same phenomenon is the basis for triple-stranded collagen molecules that are denatured by heat and renatured in concentrated solution to obtain permanently entangled gel networks used as photographic emulsions.[26]

The values of the steady-state birefringence also support the model of a rigid dimer structure that undergoes an order/disorder transition. The steady

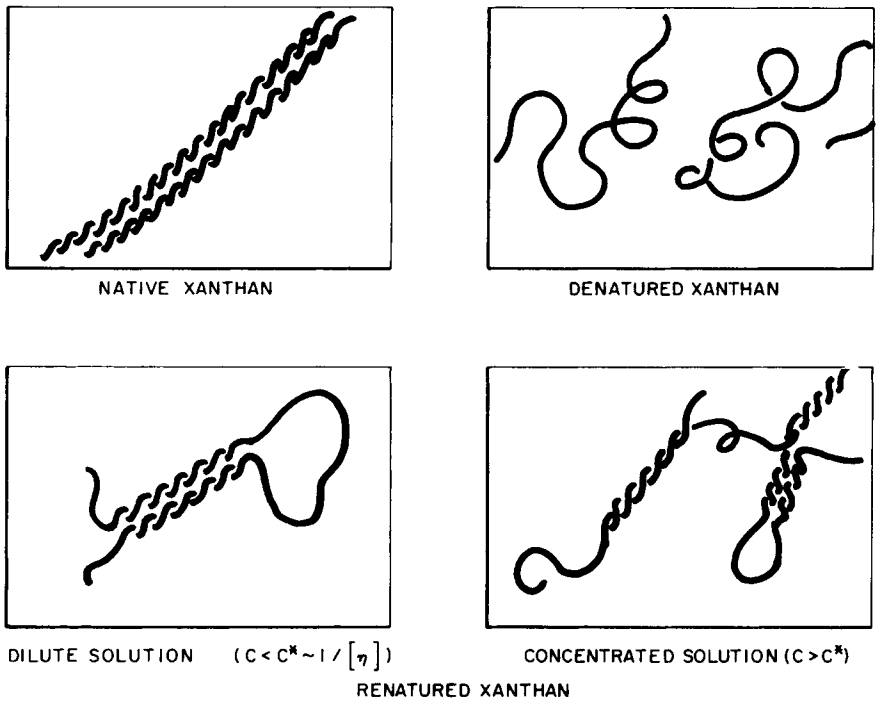

Fig. 5. Schematic representation of native, denatured, and renatured xanthan. The effect of solution concentration on aggregate formation in renatured solution is shown.

state birefringence of the native xanthan, $\Delta n = 7.62 \times 10^{-9}$ rad, is higher than that of the denatured xanthan, $\Delta n = 3.12 \times 10^{-9}$ rad, or renatured xanthan, $\Delta n = 5.67 \times 10^{-9}$ rad. The helical backbone structure, whether it is a single or double helix, would have a higher birefringence than the disordered, denatured xanthan. However, the renatured xanthan, if it were a single helix, would be expected to have the same birefringence as the native xanthan. But it is observed that the renatured xanthan has an appreciably lower steady state birefringence. The birefringence might have been lowered due to chain degradation during heating; however, heating under the conditions we imposed is not severe enough to degrade the xanthan,[8,9] and the longest relaxation time of the degraded material would have been shorter than that of the native material—but experimentally we observed that the relaxation time increased. Rather, the decrease in birefringence for the renatured material supports Holzwarth and Prestridge's[13] and Sato's[15,16] conclusions that the xanthan dimer or double helix renatures to a dimer or double helix but that imperfections are introduced in the helix or dimer structure. The ORD measurement, apparently, is not sensitive enough to detect the few imperfections that are introduced during renaturation. This has led to the (incorrect) conclusion[2] that no hysteresis occurs upon heating and cooling. Our more sensitive birefringence measurements show that, though the bulk of the backbone renatures back into a helix, the few imperfections introduced can substantially alter the large-scale configuration of the molecule.

Our results can be compared with two birefringence studies of xanthan.[22,23] Morris et al.[22] used dry xanthan to prepare heat-denatured samples in 4*M* urea *without added salt.* They analyzed their data using the initial slope (which we have critiqued in the discussion above) to obtain a relaxation time of 4 ms for concentrations between 200 and 800 ppm. They did not analyze the long-time behavior of their relaxation curves. Their values are larger than those we report probably because, without the added salt, polyelectrolyte coil expansion is greater for their samples than for ours. Ross-Murphy et al.[23] studied xanthan samples dissolved in either 0.02% sodium azide or 0.02% sodium azide with 4*M* urea. Both solutions with 600 ppm xanthan concentrations were heated to 90°C and correspond to our "renatured" and "denatured" samples, respectively. Their results for these two solutions are consistent with ours, but they could not quantify their observations as we can. They observed that for the renatured samples (in 0.02% sodium azide) the solutions could only be filtered through 0.22 μm filters with difficulty—indicating the presence of aggregates. The urea treated "denatured" samples were easily filtered. Even after filtration their renatured sample relaxed more slowly than the denatured sample (see their Fig. 5.) Since their renaturing occurred at higher concentrations (600 ppm) than in our study (100 ppm) it would be expected that the aggregates would be larger. They note that 5% of the renatured xanthan was lost during filtration indicating a substantial population of large aggregates.

CONCLUSIONS

We believe that these electric birefringence measurements provide further evidence that xanthan exists in its native form as a rigid dimer or double stranded helix. The electric birefringence evidence comes from both the level of birefringence and the relaxation times. Like Holzwarth's electron microscopy results, and Sato's light scattering results in two different solvents, the measurements do not involve mathematical models that must be invoked to relate two measured quantities. The conclusions come from the direct interpretation of each part of the electric birefringence signal.

Further, the ability to create a xanthan solution with a longer relaxation time (which also means higher viscosity) by thermal processing is most intriguing. It suggests that more work on the effect of polymer concentration on the aggregate size produced during renaturing should be investigated. This also suggests the origin of "microgels" that occur when dried samples are dissolved. These microgels have profound effects on the filtration of xanthan solutions and the injection of xanthan solutions into porous media in oil recovery operations.

We wish to thank American Cyanamid Co. for financial support, and Mr. Paul Westkaemper for assistance with data analysis.

APPENDIX: ANALYSIS OF BIREFRINGENCE DATA

A straightforward way of analyzing optical systems which employ polarized light is through the use of the Stokes vector and Mueller matrices, the so-called Mueller–Stokes calculus.[27] An excellent discussion of this technique is presented by Shurcliff.[28]

The Stokes vector describes the intensity and state of polarization of a beam of light. The Mueller matrices represent the optical components which act on the polarized beam to change its polarization state. The Mueller matrices for the elements in the birefringence apparatus are:

$$M_P = \tfrac{1}{2}\begin{bmatrix} 1 & 0 & 1 & 0 \\ 0 & 0 & 0 & 0 \\ 1 & 0 & 1 & 0 \\ 0 & 0 & 0 & 0 \end{bmatrix} \tag{2}$$

for an ideal homogeneous linear polarizer with its optic axis at 45° (the polarizer),

$$M_A = \tfrac{1}{2}\begin{bmatrix} 1 & 0 & -1 & 0 \\ 0 & 0 & 0 & 0 \\ -1 & 0 & 1 & 0 \\ 0 & 0 & 0 & 0 \end{bmatrix} \tag{3}$$

for an ideal homogeneous linear polarizer with its optic axis at $-45°$ (the analyzer), and

$$M_S = \begin{bmatrix} 1 & 0 & 0 & 0 \\ 0 & 1 & 0 & 0 \\ 0 & 0 & \cos\delta & \sin\delta \\ 0 & 0 & -\sin\delta & \cos\delta \end{bmatrix} \tag{4}$$

for an ideal homogeneous linear retarder (i.e., bifringence sample) with its optic axis at 0°.

The arrangement of the optical elements for the birefringence apparatus is shown in Figure 2. The optical axes are defined by the electric field which is parallel to the x-coordinate and the axis of molecular orientation.

Combining the above matrices by multiplication yields the following matrix for the system:

$$M_{\text{system}} = M_A \times M_S \times M_p$$

$$= \tfrac{1}{4}\begin{bmatrix} 1-\cos\delta & 0 & 1-\cos\delta & 0 \\ 0 & 0 & 0 & 0 \\ -1+\cos\delta & 0 & -1+\cos\delta & 0 \\ 0 & 0 & 0 & 0 \end{bmatrix} \tag{5}$$

The Stokes vector of the beam emerging from the analyzer (the detected beam) is given by:

$$S_0 = M_{\text{system}} \times S_i \tag{6}$$

where S_0 is the emerging beam, S_i is the incident beam, and M_{system} is the previously defined system Mueller matrix.

If the incident beam is described as having arbitrary intensity I_0 and unknown polarization, its Stokes vector would be

$$S_i = I_0\begin{bmatrix} 1 \\ a \\ b \\ c \end{bmatrix} \tag{7}$$

The emerging beam would then have the Stokes vector:

$$S_0 = \frac{I_0}{4}\begin{bmatrix} 1-\cos\delta & 0 & 1-\cos\delta & 0 \\ 0 & 0 & 0 & 0 \\ -1+\cos\delta & 0 & -1+\cos\delta & 0 \\ 0 & 0 & 0 & 0 \end{bmatrix}\begin{bmatrix} 1 \\ a \\ b \\ c \end{bmatrix}$$

$$= \frac{I_0(1+b)}{4}\begin{bmatrix} 1-\cos\delta \\ 0 \\ -1+\cos\delta \\ 0 \end{bmatrix} \tag{8}$$

The intensity of the beam is given by the first element of the Stokes vector

$$I_\delta = KI_0(1 - \cos\delta) \tag{9}$$

$$= 2KI_0 \sin^2(\delta/2) \tag{10}$$

where

$$K = (1 + b)1/4 \tag{11}$$

The value of the proportionality constant K can be measured experimentally. With all components in place, the analyzer is rotated so that its optical axis is equal to some angle α. With the electric field off, and δ subsequently equal to zero, the Mueller matrix for the system is

$$M_{\text{system}} = \tfrac{1}{4}\begin{bmatrix} 1 + \sin 2\alpha & 0 & 1 + \sin 2\alpha & 0 \\ \cos 2\alpha + \cos 2\alpha \sin 2\alpha & 0 & \cos 2\alpha + \cos 2\alpha \sin 2\alpha & 0 \\ \sin 2\alpha + \sin^2 2\alpha & 0 & \sin 2\alpha + \sin^2 2\alpha & 0 \\ 0 & 0 & 0 & 0 \end{bmatrix} \tag{12}$$

This results in a Stokes vector of

$$S_0 = \frac{I_0(1 + b)}{4}\begin{bmatrix} 1 + \sin 2\alpha \\ \cos 2\alpha(1 + \sin 2\alpha) \\ \sin 2\alpha(1 + \sin 2\alpha) \\ 0 \end{bmatrix} \tag{13}$$

[assuming the incident Stokes vector given in eq. (7)]. Therefore, the resulting intensity is

$$I_\alpha = KI_0(1 + \sin 2\alpha) \tag{14}$$

By rotating the polarizer to various angles α and measuring the intensity of the emerging beam I_α the proportionality constant KI_0 may be measured. The constant K accounts for reflections and absorption losses that attenuate the intensity of the incident light as it passes through the optical train. The birefringence Δn is calculated from the retardation δ by employing the definition of birefringence

$$\Delta n = \lambda\delta/2\pi l \tag{15}$$

where l is the optical pathlength of the sample and λ is the wavelength of light. We finally obtain, by combining eq. (15) and (10):

$$\Delta n = \frac{\lambda}{\pi l}\sin^{-1}\left(\frac{I_\delta}{2KI_0}\right)^{1/2} \tag{16}$$

For small values of δ, such as we find for dilute polymer solutions, the sine function [eq. (10)] can be expanded in a Taylor series to obtain:

$$I_\delta \approx 2KI_0\left[\frac{\delta^2}{4} + O(\delta^3)\right] \tag{17}$$

and

$$\Delta n \approx \frac{\lambda}{\pi l}\left(\frac{I_\delta}{2KI_0}\right)^{1/2} \tag{18}$$

The birefringence decay is assumed to follow a sum of exponentials form:

$$\Delta n = \sum_i A_i e^{-t/\tau_i} \tag{19}$$

Therefore, combining eqs. (18) and (19) for the longest relaxation time (i.e., a single term in the series) and taking the logarithm, we find

$$\ln I_\delta \doteq \ln\left(\frac{A_1 \pi l \sqrt{2KI_0}}{\lambda}\right)^2 - \frac{2t}{\tau_1} \tag{20}$$

Equation (20) shows that plotting the logarithm of I_δ [or equivalently the logarithm of the detector response when KI_0 includes the calibration obtained using eq. (14)] vs. t results in a line of slope $-2/\tau_1$ and intercept $2KI_0(A_1\pi\ell/\lambda)^2$ from which A_1 can be determined since the other parameters are known.

References

1. A. Jeanes, J. E. Pittsley, and F. R. Senti, *J. Appl. Polym. Sci.*, **5**, 519–526 (1961).
2. M. Milas and M. Rinaudo, *Carbohydrate Res.*, **76**, 189–196 (1979).
3. M. Rinaudo and M. Milas, *Biopolymers*, **17**, 2663–2678 (1978).
4. G. Holzwarth, *Div. Pet. Chem., Prepr., Am. Chem. Soc.*, **21**, 281–296 (1976).
5. G. Chauveteau and N. Kohler, Soc. of Petroleum Engineers, SPE #9295, presented at 55th Annual Fall Tech. Conf. of SPE, Dallas, TX, Sep. 1980.
6. P. J. Whitcomb and C. W. Macosko, J. Rheol., **22**, 493–505 (1978).
7. J. C. Phillips, J. W. Miller, W. C. Wernau, B. E. Tate, and M. H Auerbach, Soc. of Petroleum Engineers, SPE #10617, presented at SPE 6th Int. Symp. on Oilfield and Geothermal Chem., Dallas, TX, Jan. 1982.
8. C. Chen and E. W. Sheppard, *J. Macromol. Sci Chem.*, **A13**, 239–259 (1979).
9. C. Chen and E. W. Sheppard, *Polym. Eng. and Sci.*, **20**, 512–516 (1980).
10. T. Lim, J. T. Uhl and R. K. Prud'homme, *J. Rheol.*, **28**(4), 367–379 (1984).
11. R. Moorhouse, M. D. Walkinshaw, and S. Arnott, "Xanthan Gum—Molecular Conformation and Interactions," in *Extracellular Microbial Polysaccharides*, P. A. Sandford and A. I. Laskin, Eds., ACS Symp. Ser. No. 45, Am. Chem. Soc., Washington, DC, 1977.
12. G. Muller, L. Lecourtier, G. Chauveteau, and C. Allain, *Makromol. Chem., Rapid Commun.*, **5**, 203–208 (1984).
13. G. Holzwarth and E. B. Prestridge, *Science*, **1977** 197.
14. G. Paradossi and D. A. Brant, Macromol., **15**, 874–879 (1982).
15. T. Sato, T. Norisuye, and H. Fujita, *Polym. J.*, **16**(4), 341–350 (1984).
16. T. Sato, S. Kojima, T. Novisuye, and H. Fujita, *Polym. J.*, **16**(5), 423–429 (1984).
17. G. Holzwarth, *Biochemistry*, **15**, 4333–4339 (1976).
18. N. Kohler and G. Chauveteau, Society of Petroleum Engineers, SPE #7425, 53rd Annual SPE Fall Meeting, 1978.
19. Flocon Biopolymer 4800, Technical Brochure, Pfizer Inc., Groton, CT.
20. A. M. Jamieson, J. G. Southwick, and J. Blackwell, *J. Polym. Sci. Polym. Phys. Ed.*, **20**, 1513 (1982).
21. R. L. Jernigan and D. S. Thompson, *Molecular Electro-Optics, Part I*, C. T. O'Konski, Ed., Marcel Dekker, New York, 1976, Chap. 5.
22. V. J. Morris, K. l'Anson, and C. Turner, *Int. J. Biol. Macromol.*, **4**, 362–366 (1982).
23. S. B. Ross-Murphy, V. J. Morris, and E. R. Morris, *Faraday Symp. Chem. Soc.*, **18**, 115–130 (1983).
24. C. T. O'Konski, Ed., *Molecular Electro-Optics*, Part I and II, Marcel Dekker, New York, 1976.
25. D. A. Hoagland, Ph.D. thesis, Department of Chemical Engineering, Princeton University, Princeton, NJ, 1986.
26. I. V. Yannas, *Rev. Macromol. Chem.*, **C7**, 49–104 (1972).
27. P. S. Hauge, R. H. Muller, and C. G. Smith, *Surface Sci.*, **96**(1–3), 81–107 (1980).
28. W. A. Shurcliff, *Polarized Light*, Harvard Univ. Press, Cambridge, MA, 1962, Appendix 2.